

Synthesis and Characterization of Star-Shaped Poly(ethylene-*co*-propylene) Polymers Bearing Terminal Self-Complementary Multiple Hydrogen-Bonding Sites

Casey L. Elkins, Kalpana Viswanathan, and Timothy E. Long*

Department of Chemistry, Macromolecules and Interfaces Institute (MII), Virginia Polytechnic Institute and State University, Blacksburg, Virginia 24061-0344

Received December 26, 2005; Revised Manuscript Received February 28, 2006

ABSTRACT: The polymerization of isoprene was initiated with 3-(*tert*-butyldimethylsilyloxy)-1-propyllithium (TBDMSPrLi), which contained a silyl-protected hydroxyl functionality. Living poly(isoprenyllithium) with controlled molecular weight and narrow molecular weight distribution coupled efficiently with divinylbenzene to form well-defined star-shaped polymers. Both linear and star-shaped polymers were subsequently hydrogenated to poly(ethylene-*co*-propylene) and deprotected quantitatively to yield terminal primary hydroxyl functionality. High conversions of hydroxyl functionality to the 2-ureido-4[1*H*]-pyrimidinone (UPy) quadruple hydrogen-bonding group were achieved using isocyanate coupling and subsequent reaction with 6-methylisocytosine. Nonfunctionalized and UPy-functionalized linear and star-shaped poly(ethylene-*co*-propylene)s were characterized using ¹H NMR spectroscopy, dynamic mechanical analysis (DMA), differential scanning calorimetry (DSC), tensile testing, and melt rheology. The observed glass transition temperatures were independent of molecular architecture for the UPy-functionalized polymers and nonfunctionalized analogues using both DSC and DMA. Tensile testing revealed the UPy-functionalized star polymers (UPy-Star) exhibited a higher Young's modulus and lower percent elongation at failure compared to the UPy-telechelic polymers with *M_n* of 24 000 g/mol (UPy-24K-T) analogues. UPy-Star polymer exhibited a rubbery plateau region over a well-defined frequency range, and in contrast, the UPy-functionalized linear polymers were in the terminal flow regime, which suggested greater association for the star-shaped polymers. In addition, complex viscosity data revealed a non-Newtonian behavior for the star-shaped polymers in contrast to linear analogues, which is also consistent with a highly associated structure.

Introduction

The introduction of branching dramatically influences polymer physical properties and melt processability.^{1–4} Long chain branching generally alters rheological and processing performance, while short chain branching influences thermal and mechanical solid-state behavior. Although long chain branching significantly influences polymer physical properties, a fundamental understanding of structure–property relationships remains difficult due to the complexity of branched polymer architectures. Star-shaped macromolecules, which contain only one branch point, are a more simplified model of branched macromolecules and have received significant attention in the elucidation of structure–property relationships.^{5–11} Although star polymers constitute the simplest branched structure, the synthesis of star-shaped polymers remains challenging, and well-defined star polymers are often difficult to prepare in a controlled manner. Moreover, chain-end functionalization is an additional challenge in the synthesis and characterization of telechelic star-shaped polymers.

Controlled polymerization techniques, such as living anionic,^{12–20} cationic,^{21–28} free radical,^{29–33} and group transfer polymerization,^{34–37} were reported earlier for the preparation of well-defined star-shaped macromolecules. Living anionic polymerization methodologies coupled with functionalized alkylolithium initiators were also used earlier to synthesize well-defined chain-end-functionalized polymers in various architectures. The use of functionalized anionic initiators has several advantages over more traditional electrophilic termination reagents for the synthesis of telechelic polymers.³⁸ Each

functionalized initiator molecule ensures a macromolecule with the desired functionality at the chain end regardless of molecular weight. The use of functionalized initiators avoids problems associated with electrophilic termination reagents, such as efficient and rapid mixing with viscous polymer solutions, stability of the anionic chain end, and selective reactivity.³⁹ Functionalized initiators also facilitate the synthesis of telechelic and heterotelechelic polymers, functionalized block polymers, and star-shaped polymers with functional groups on each arm terminus.⁴⁰ The use of the functional initiator 3-(*tert*-butyldimethylsilyloxy)-1-propyllithium (TBDMSPrLi) was reported in the synthesis of a variety of polymers with various molecular architectures, including polyisoprene,^{38,41–44} polybutadiene,^{38,40,41,44,45} poly(methyl methacrylate),^{46,47} and poly(1,3-cyclohexadiene),⁴⁸ to yield hydroxyl chain-end-functionalized polymers.

Although living anionic polymerization in combination with functional initiation has proven an excellent route to telechelic linear and star-shaped polymers, telechelic star-shaped macromolecules were also reported using various other methodologies. Hedrick et al. reported the core-first synthesis of star-shaped poly(ϵ -caprolactone) hydroxyl-terminated macroinitiators with six arms using ring-opening polymerization and the subsequent transformation into atom transfer radical polymerization (ATRP) initiators.⁴⁹ The macroinitiators were then used to polymerize several monomers, including methyl methacrylate, hydroxyethyl methacrylate, and ethylene oxide. In a similar fashion, Gnanou and co-workers used living cationic polymerization to synthesize star-shaped polystyrenes and transformed the peripheral chain-end functionality into either a hydroxyl or amine group.⁵⁰ The hydroxyl-terminated samples were used as macroinitiators for

* To whom correspondence should be addressed: e-mail telong@vt.edu.

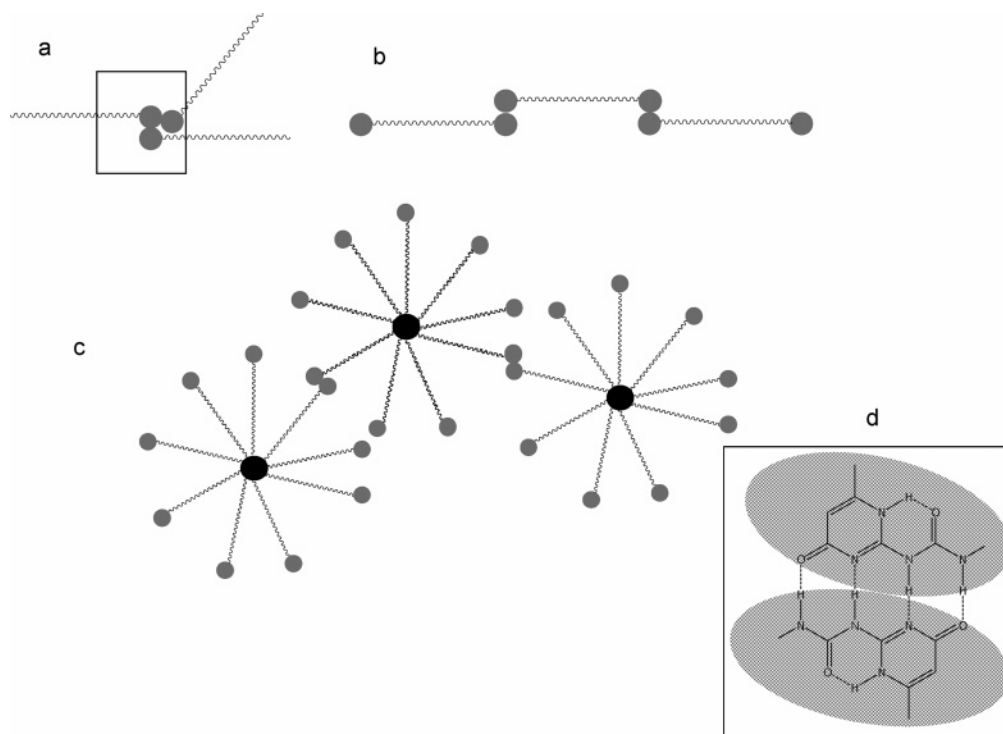


Figure 1. Illustration of the self-assembly of (a) linear monofunctional, (b) linear telechelic, and (c) star polymers through quadruple hydrogen bonding between UPy groups as shown in (d). For simplicity, only dimeric association between the chain ends are represented, while in a solution the chain ends may interact with multiple groups to form an aggregated structure.

ethylene oxide polymerization. In several cases, ATRP was used in acrylic polymerizations to yield hydroxyl-,⁵¹ epoxy-,⁵¹ amino-, bromide-, or cyano-functionalized star polymers.⁵² Quirk et al. also introduced functionality to star-shaped polymers using living anionic polymerization in conjunction with functionalized diphenylethylene derivatives and organic functional group transformations.^{15,39,53} and Hirao et al. subsequently based their efforts on this methodology.^{54–56} Quirk was able to introduce functionality at either the α -terminus, block junctions, or core.

Fréchet and Hawker et al. recently reported the use of nitroxide-mediated polymerization in the synthesis of functionalized star polymers.⁵⁷ Using a modular approach, a library of compounds was synthesized with various compositions, including homo, block, and random copolymers with both apolar and polar vinylic repeat units and functional groups. Ishizu et al. also reported the functionalization of polyisoprene star polymers with *p*-chloromethylstyrene to yield a periphery of reactive styrene groups, which were capable of subsequently forming a cross-linked network.⁵⁸

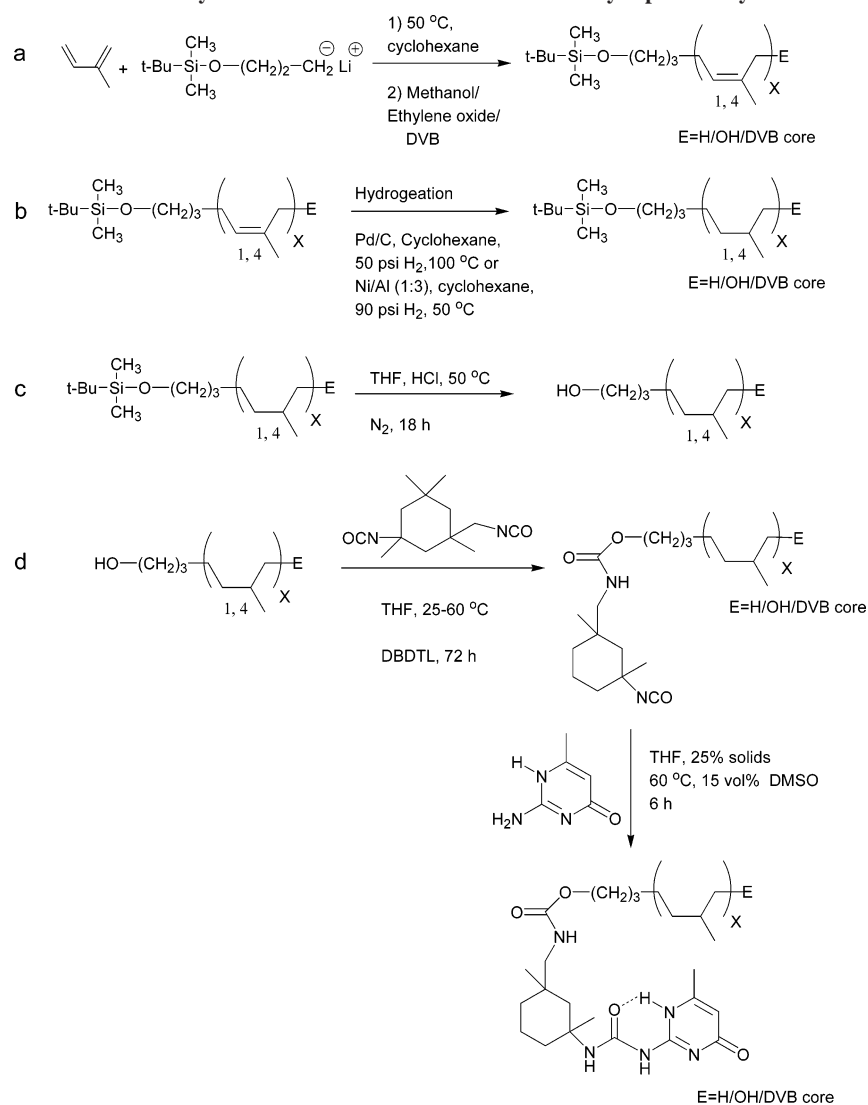
Although both functional polymers and star-shaped polymers are prevalent in the literature, the combination of well-defined thermoreversible chain-end interactions, such as multiple hydrogen-bonding interactions, and star-shaped macromolecules is limited. Hadjichristidis et al. studied the synthesis and characterization of well-defined linear and star-shaped polystyrenes, polyisoprenes, and polybutadienes bearing sulfo- and phosphoro-zwitterionic groups capable of thermoreversible association.^{59–65} Although these studies contributed significantly to the understanding of structure–property relationships, the reversible interaction is electrostatic, and the behavior of polymers that interact through multiple hydrogen bonding is expected to differ significantly. Meijer et al. recently reported the synthesis of model low-molecular-weight poly(ethylene oxide-*co*-propylene oxide) three-arm star-shaped polymers with pendant 2-ureido-4[1H]-pyrimidinone (UPy) quadruple hydrogen-bonding functionalities.⁶⁶ These polymers were compared with

three-arm star-shaped polymers bearing urea chain ends, non-functional chain ends, and a chemically cross-linked network.

Previous research in our laboratories involved the synthesis of linear polystyrenes, polyisoprenes, microphase-separated polystyrene-*block*-polyisoprene copolymers, and polyesters with chain-end multiple hydrogen-bonding sites. The influence of multiple hydrogen bond incorporation on physical properties was investigated using glass transition temperature, melt viscosity, and morphology.^{67–69} This paper will focus on the effects of multiple hydrogen-bonding and polymer topology on mechanical, thermal, and rheological properties of relatively nonpolar star-shaped macromolecules. Living anionic polymerization, which was initiated with TBDMSPrLi, was a facile synthetic methodology for the preparation of well-defined polymers with two different chain ends (nonfunctionalized and UPy-functionalized) in three molecular architectures, i.e., linear monofunctional, linear telechelic functional, and star-shaped with functionality at each arm terminus. The UPy-promoted association between polymer chains of various topologies is illustrated in Figure 1.

Experimental Section

Materials. Isoprene (Aldrich, 99%) was passed through an alumina column and a molecular sieves column. Nickel octoate (Shepherd Chemicals, 8% (w/w) in mineral spirits), triethylaluminum (Aldrich, 1.4 M in hexane), palladium on activated carbon (Aldrich, 10% (w/w)), 3-(*tert*-butyldimethylsilyloxy)-1-propyl-lithium (TBDMSPrLi, FMC Corp. Lithium Division, 0.4 M in cyclohexane), ethylene oxide (Aldrich), dimethyl sulfoxide (Aldrich, anhydrous grade), and isophorone diisocyanate (IPDI) (Aldrich, 98%) were used as received. Divinylbenzene (DVB) (Aldrich, 80% divinylbenzene comprising a mixture of isomers, 20% ethylvinylbenzene) was stirred over calcium hydride for 24 h, degassed several times, and vacuum-distilled (0.10 mmHg, 23–25 °C). Divinylbenzene was then vacuum-distilled from dibutylmagnesium (0.10 mmHg, 23–25 °C). Cyclohexane (EM Science, ACS grade) was passed through an alumina column and a molecular sieves column

Scheme 1. Synthesis of Chain-End-Functionalized Polyisoprene Polymers^a

^a The polymer product contains both 1,4- and 3,4-enchainment. However, for simplicity, only the 1,4-microstructure is shown, where DVB = divinylbenzene, DBDTL = dibutyl tin dilaurate, DMSO = dimethyl sulfoxide, and E = polymer end group. E is H when terminated with methanol to yield monofunctional polymer, E is OH when terminated with ethylene oxide to yield telechelic polymer, and E is a DVB core when terminated with DVB to yield star polymer.

immediately prior to use. Tetrahydrofuran (THF) (EM Science, HPLC grade) was distilled from sodium/benzophenone immediately prior to use. Dibutyl tin dilaurate (DBDTL) (Aldrich, 99%) was dissolved in THF as a 1 wt % solution. 6-Methylisocytosine (MIC) (Aldrich, 98%) was dried at 100 °C under vacuum overnight to remove moisture impurity.

Synthesis of Linear Telechelic Polyisoprene. All polymerizations were conducted using a glass anionic reactor system, which consisted of a 600 mL heavy-walled, glass bowl, a stainless steel top plate, and stainless steel magnetically coupled mechanical stirrer. In addition to this basic assembly, the unit was equipped with a heat-exchange coil, a thermocouple, a thermistor to measure and control the temperature, a septum sealed port and various stainless steel transfer lines to introduce isoprene (monomer) and cyclohexane (solvent), and inlet/vent for purified nitrogen. The temperature was controlled using steam/cold water passed through stainless steel coils within the 600 mL glass polymerization vessel. The system was maintained at a constant nitrogen pressure (10–15 psi).

The 600 mL reaction vessel was charged with cyclohexane (500 mL, 4.64 mol) and isoprene (45 mL, 0.44 mol) and maintained at 50 °C. TBDMSPrLi (4.47 mL, 2 mmol) was added to the solution to initiate polymerization, targeting a 15 000 g/mol polymer. The reaction was allowed to proceed for 2 h to ensure quantitative conversion. Degassed methanol was added to terminate the polymer-

ization and generate monofunctional polyisoprenes. An excess of ethylene oxide was bubbled through the polymerization solution and allowed to react for 30 min to prepare telechelic polyisoprenes. The polymerization was terminated using degassed methanol, as depicted in Scheme 1a. ¹H NMR (400 MHz, CDCl₃, δ): 5.1 ppm (b, 1,4-polyisoprene), 4.75 ppm (b, 3,4-polyisoprene), 3.6 ppm (t, CH₂-O-Si(CH₃)₂(C(CH₃)₃), 1.0–2.2 (b, -CH₃, -CH₂-, CH in polyisoprene units), 0.9 ppm (s, CH₂-O-Si(CH₃)₂(C(CH₃)₃), 0.04 ppm (s, CH₂-O-Si(CH₃)₂(C(CH₃)₃). Monomer conversion was greater than 90%, and ¹H NMR indicated that the microstructure of the polymer was approximately 92% 1,4-enchainment and 8% 3,4-enchainment.

Synthesis of Star-Shaped Telechelic Polyisoprene. The 600 mL reaction vessel was charged with cyclohexane (500 mL, 4.64 mol) and isoprene (45 mL, 0.44 mol) and maintained at 50 °C. TBDMSPrLi (4.47 mL, 2 mmol) was added to the solution to initiate polymerization, targeting a 15 000 g/mol polymer. The reaction was allowed to proceed for 2 h. After 2 h, an aliquot was removed and terminated with degassed methanol. DVB (1.89 mL, 10.7 mmol) was added to the solution to couple the polyisoprene arms. The reaction was allowed to proceed overnight. The reaction was terminated via the addition of degassed methanol as depicted in Scheme 1a. ¹H NMR assignments corresponded to those from linear polyisoprene and resonances for divinylbenzene were not

observed, presumably due to immobility in the star core. Monomer conversion was greater than 90%, and SEC indicated greater than 95% coupling of the arms to star polymer.

Hydrogenation of Polyisoprene Linear Polymers. A linear polyisoprene (18 g) was dissolved in cyclohexane (110 mL) and added to a 500 mL pressure vessel. Pd/C (2.5 g) catalyst was added, and the reactor was pressurized with hydrogen and vented three times. The vessel was pressurized with hydrogen (50 psi) and heated to 100 °C for 24 h, as depicted in Scheme 1b. The Pd/C catalyst was removed using filtration through Celite. The cyclohexane solution was concentrated to 100 mL in vacuo. The polymer solution was then precipitated into 2-propanol (600 mL) and dried in vacuo at 60 °C for 24 h. ¹H NMR (400 MHz, CDCl₃, δ): 3.6 ppm (t, CH₂-O-Si(CH₃)₂(C(CH₃)₃), 1.0–2.0 (b, -CH₃, -CH₂-, CH in poly(ethylene-co-propylene) units), 0.9 ppm (s, CH₂-O-Si(CH₃)₂(C(CH₃)₃), 0.04 ppm (s, CH₂-O-Si(CH₃)₂(C(CH₃)₃)). The yield, which was determined gravimetrically, was between 60% and 85%, and ¹H NMR indicated complete hydrogenation.

Synthesis of Preformed Nickel Hydrogenation Catalyst. The alternate nickel hydrogenation catalyst was synthesized as previously described.⁷⁰ Cyclohexane (15 mL) and nickel octoate (0.228 g, 0.66 mmol) were added to a septum-sealed 100 mL round-bottomed flask purged with nitrogen. Triethylaluminum (TEA) (1.36 mL, 9.9 mmol) was added dropwise to the nickel solution. An opaque, black colloidal suspension formed immediately and was allowed to age for 15 min at room temperature under a nitrogen atmosphere to form a homogeneous solution.

Hydrogenation of Polyisoprene Star-Shaped Polymers. A polyisoprene star polymer (3.0 g, 0.02 mmol) and a preformed nickel catalyst (~20 mL, 0.10 mmol) were dissolved in cyclohexane (500 mL) and added to a 600 mL reactor. The reactor was pressurized with hydrogen and vented three times. The vessel was pressurized with hydrogen (90 psi) and heated to 50 °C for 24 h, as summarized in Scheme 1b. The nickel catalyst was extracted from the polymer solution with three citric acid (Aldrich, 98%, 500 mL, 50 mmol) washes following quantitative hydrogenation. The cyclohexane solution was concentrated to 100 mL, precipitated into 2-propanol (600 mL), and dried in vacuo at 60 °C for 24 h. ¹H NMR assignments corresponded to those of hydrogenated linear polyisoprene. Quantitative hydrogenation of the arms was confirmed by ¹H NMR spectroscopy, and the recovered yield was 84%.

Removal of Protecting Group from Poly(ethylene-co-propylene). The poly(ethylene-co-propylene) (1.0 g, 0.007 mmol) was dissolved in THF (50 mL), and concentrated hydrochloric acid (10 M, 5 mL) was added to the solution. The solution was allowed to stir for 18 h at 50 °C and precipitated into 2-propanol twice to remove residual hydrochloric acid. The polymer was then dried at 60 °C under vacuum for 24 h, as depicted in Scheme 1c. ¹H NMR (400 MHz, CDCl₃, δ): 3.6 ppm (t, CH₂-OH), 1.0–2.0 (b, -CH₃, -CH₂-, CH in poly(ethylene-co-propylene) units). ¹H NMR confirmed complete deprotection of the hydroxyl groups with an isolated yield of ~85%.

Functionalization of Polymers with UPy Groups. After quantitative deprotection of poly(ethylene-co-propylene) was achieved, the UPy terminal group was attached in two steps. In the first step, the poly(ethylene-co-propylene) (1.0 g, 0.007 mmol) was dissolved in freshly distilled THF (3.5 mL), and DBDTL catalyst (0.01 mL, 0.017 mmol) was added. IPDI (0.29 mL, 1.36 mmol) was added to the solution, and reaction was allowed to proceed for 72 h at 60 °C to ensure complete conversion. In the second step, MIC (0.38 g, 3 mmol) was added under nitrogen flush, and anhydrous DMSO (0.5 mL) was added as a cosolvent. The reaction proceeded under nitrogen at 60 °C for 72 h. The reaction solution was quenched using excess methanol and filtered in order to isolate the polymer. The product was dissolved in chloroform and filtered again in order to remove residual MIC. The polymer was precipitated into methanol, collected, and dried in vacuo. The complete series of polymers and nonfunctionalized analogues is summarized in Table 2. Residual MIC, IPDI, and coupled products were quantitatively removed through repeated filtration and selective solvent precipita-

Table 1. Molecular Weight Control Using TBDMSPrLi as Initiator for the Anionic Polymerization of Isoprene

M_n (target) (g/mol)	M_n (SEC) ^a (g/mol)	M_n (NMR) ^b (g/mol)	M_w/M_n ^a	T_g (°C) ^c
5 000	4 300	4 300	1.04	-64
10 000	10 900	9 100	1.04	-65
20 000	18 600	19 100	1.04	-61
47 000	49 900	52 100	1.06	-62

^a Determined using SEC at 40 °C in THF with a MALLS detector.

^b Determined using a Varian 400 MHz NMR spectrometer at 25 °C in CDCl₃. ^c Determined using a Perkin-Elmer Pyris 1 cryogenic DSC at a heating rate of 20 °C/min under nitrogen.

tion. ¹H NMR (400 MHz, CDCl₃, δ): 12.9–13.2 (s, -NH-C(CH₃)- in UPy units), 11.8–12.1 (s, -NH-C-N- in UPy units), 10.4–10.7 (s, -CH₂NH-CO- in UPy units), 5.7–6.0 (s, NHC(CH₃)-CHO- in UPy units), 1.0–2.0 (b, -CH₃, -CH₂-, CH in poly(ethylene-co-propylene) units). Following the two-step functionalization, the recovered yield was between 80% and 85%, and ¹H NMR indicated 75–100% functionalization of the hydroxyl groups with the UPy units.

Characterization. ¹H NMR spectra were collected in CDCl₃ at 400 MHz with a Varian Unity spectrometer. Glass transition and melting temperatures were determined using a Perkin-Elmer Pyris 1 cryogenic differential scanning calorimeter (DSC) at a heating rate of 20 °C/min under nitrogen, which was calibrated using indium (mp = 156.60 °C) and zinc (mp = 419.47 °C). Glass transition temperatures are reported as the transition midpoint during the second heat. Molecular weights were determined at 40 °C in THF (HPLC grade) at 1 mL/min using polystyrene standards on a Waters 717+ autosampler size exclusion chromatograph (SEC) equipped with three in-line 5 μm PLgel MIXED-C columns, a Waters 2410 refractive index (RI) detector operating at 880 nm, and a Wyatt Technologies miniDAWN multiple angle laser light scattering (MALLS) detector operating at 690 nm, which was calibrated with polystyrene standards. The refractive index increment (dn/dc) was calculated online. All molecular weight values reported are absolute molecular weights obtained using the MALLS detector. SEC analysis was not reliable for star-shaped UPy functional polymers due to their association at SEC concentrations in THF, which was verified using dynamic light scattering. Melt rheological analysis was used for the determination of storage moduli and complex viscosities of the nonfunctionalized and UPy-functionalized polymers. Melt rheology was performed on a TA Instruments AR2000 stress-controlled rheometer. A 25 mm parallel plate geometry was used, and rheological analysis was performed at a 5% strain amplitude over a frequency range of 1–100 Hz. Comparison between linear nonfunctionalized and UPy-functionalized polymers was performed at 50 °C, while comparison with UPy-star polymers was performed at 100 °C. A comparison of peak height vs a common baseline point was performed to eliminate data scatter due to baseline drift. Stress-strain experiments were performed using dogbone-shaped film samples ($n = 6$) cut using a die according to ASTM D3368. The tensile tests were performed under ambient conditions on a 5500R Instron universal testing machine at a crosshead displacement rate of 10 mm/min. Stress vs strain profiles were recorded using Merlin software at an acquisition rate of 50 ms per each data point. Pneumatic grips were used, and no slippage was observed. DMA experiments were performed with a TA Instruments DMA 2980 dynamic mechanical analyzer in tension mode at a frequency of 1 Hz. The temperature ramp was 3 °C/min.

Results and Discussion

Polymer Synthesis. The polymerization of isoprene was controlled using the protected hydroxyl initiator, TBDMSPrLi, and homopolymers with narrow molecular weight distributions were obtained (Table 1). Subsequent end-capping with ethylene oxide and termination with methanol produced telechelic functional polymers. Polyisoprene star polymers were also

Table 2. Molecular Weight and Molecular Weight Distribution of Monofunctional, Telechelic, and Star Polyisoprene after Each Functionalization Step

polymer topology	precursor polymer $M_n (M_w/M_n)^a$	polymer $M_n (M_w/M_n)^a$ after hydrogenation ^b	polymer $M_n (M_w/M_n)^a$ after deprotection ^d	polymer $M_n (M_w/M_n)^a$ after UPy functionalization ^e
linear monofunctional	14 800 (1.04)	10 700 (1.32)	18 600 (1.04)	18 800 (1.06)
linear telechelic	11 000 (1.05)	12 600 (1.06)	12 600 (1.05)	12 200 (1.10)
	24 300 (1.08)	16 300 (1.18)	16 300 (1.19)	19 100 (1.27)
star ^c	90 700 (1.37)		87 800 (1.44)	

^a Determined using SEC at 40 °C in THF with a MALLS detector. ^b Hydrogenation conditions: cyclohexane, 50 psi H₂, Pd/C catalyst, 100 °C, 24 h, 50 psi H₂. ^c Ni/Al used as hydrogenation catalyst instead of Pd/C. ^d Deprotection conditions: THF, 1 M HCl, 50 °C, 18 h. ^e UPy functionalization conditions: THF, IPDI, DBDTL, 60 °C, 72 h; MIC, 15 mol % DMSO, 60 °C, 72 h.

Table 3. Polymer Topology, Polymer Nomenclature, % Functionalization of Poly(ethylene-co-propylene)s, and Thermal Characterization Data on the Functionalized Polymers

polymer topology	polymer nomenclature	% end-capping ^a	mol % UPy groups	T_g (°C) ^b	T_g (°C) ^c
linear monofunctional-12K	UPy-12K-mono	90	0.54	too fluid	ND
linear telechelic-12K	UPy-12K-T	95	1.14	−43	ND
linear telechelic-24K	UPy-24K-T	100	0.60	−38	−62
star	UPy-Star	75	0.45	−39	−59

^a NMR conditions: Varian Unity 400 MHz, CDCl₃, 1000 scans. ^b DMA conditions: 1 Hz, tension mode, 3 °C/min. ^c DSC conditions: Perkin-Elmer Pyris, heating rate: 10 °C/min second heat.

synthesized using the TBDMSPrLi initiator and subsequent coupling with DVB. Narrow molecular weight distributions were observed for the polyisoprene homopolymer arms prior to coupling with DVB. Relatively narrow molecular weight distributions of 1.26–1.36 were observed for the DVB coupled polyisoprene star polymers, and SEC analysis confirmed high conversion of arm precursors to star-shaped polymers. Similar microstructures were observed for polyisoprenes synthesized using either the protected hydroxyl initiator TBDMSPrLi or the more traditional *s*-butyllithium anionic initiator, and approximately 92% 1,4-enchainment and 8% 3,4-enchainment were observed in both cases. After confirming the controlled nature of isoprene polymerization with the functionalized initiator, polymers of two different targeted M_n of 12 000 and 24 000 g/mol were synthesized for further modification, as shown in Scheme 1.

Quantitative hydrogenation of the polymer was necessary to avoid deleterious acid-catalyzed coupling reactions during deprotection of the silyl-protected hydroxyl functionality. The linear polyisoprenes were quantitatively hydrogenated generally in 12 h using heterogeneous palladium/carbon catalysis, while incomplete hydrogenation of the star-shaped polyisoprenes was observed after 7–10 days under identical hydrogenation conditions. Previous literature reported hydrogenation of star-shaped polydienes at much higher temperatures (170 °C) and pressures (~800 psi),¹⁴ and a homogeneous catalyst was required to quantitatively hydrogenate the star-shaped polyisoprenes under milder reaction conditions. A homogeneous nickel octoate/triethylaluminum catalyst system provided quantitative hydrogenation of the star-shaped polymers in 12 h at moderate pressures and temperatures.

After hydrogenation, facile deprotection of the primary hydroxyl chain ends was achieved using acid catalysis. The telechelic hydroxyl-containing polymers served as well-defined precursors for the introduction of terminal multiple hydrogen-bonding functionality.

Polymer Modification with UPy Groups and Mechanical Performance. The hydroxyl chain ends of the various poly(ethylene-co-propylene)s were derivatized with UPy groups in two steps, and high conversions were achieved in all cases, as shown in Scheme 1d. The characteristic UPy ¹H NMR resonances (three NH hydrogens (10.5, 12, 13 ppm), methyne H on the pyrimidinone ring (5.8 ppm)) were compared with the aliphatic resonances of the polymer backbone (between 1

and 2 ppm) in order to determine the extent of chain end functionalization. Table 2 summarizes the molecular weight and molecular weight distribution of the polymers obtained after each functionalization step. Conversions of the hydroxyl to the UPy end group ranged from 90 to 100% for linear poly(ethylene-co-propylene)s and 75% for star-shaped polymers. Although UPy functionalization of star-shaped poly(ethylene-co-propylene)s exhibited the lowest percent functionalization, each star-shaped macromolecule contained an average of six UPy functional groups. Although UPy functionalization was not quantitative, high conversions were achieved, and the molar percentage of UPy groups is summarized in Table 3. UPy-12K-mono, UPy-24K-T, and UPy-Star polymers, for example, contained ~0.50 mol % UPy functionality; however, significantly different properties were observed for each architecture. DSC analysis indicated that the UPy functionality did not significantly change the −60 °C glass transition temperature of the precursor poly(ethylene-co-propylene) (Table 3),^{71–73} and the glass transition was the only transition observed.

Interestingly, the UPy-Star and linear UPy-24K-T polymers both formed ductile films when cast from solution, and DMA and tensile testing were used to study the mechanical performance of these films. Distinct glass transitions were observed for UPy-functionalized poly(ethylene-co-propylene)s at ~−40 °C using DMA at 1 Hz. UPy-24K-T and UPy-Star polymers exhibited a broad rubbery plateau at 3 × 10³ Pa, while UPy-12K-T exhibited a narrower rubbery plateau of the same magnitude. Unfortunately, mechanical property comparisons of nonfunctionalized counterparts were not possible because nonfunctionalized analogues were viscous liquids at room temperature and did not form free-standing films. Stress–strain profiles for the UPy-Star and linear UPy-24K-T films are shown in Figure 2. The UPy-24K-T sample ruptured at ~330% elongation and exhibited tensile properties typical of a viscous liquid under stress.⁷⁴ The UPy-Star samples, which contained similar molar concentration (~0.50 mol %) of UPy hydrogen-bonding groups, displayed a distinctly different stress–strain profile. The tensile strength for the UPy-Star films (1.06 ± 0.11 MPa) was nearly twice the UPy-24K-T films (0.56 ± 0.02 MPa), and the ~140% elongation of the UPy-Star film was lower than ~330% elongation of the UPy-24K-T film. A significant difference was observed in the Young's modulus of the UPy-24K-T (0.92 ± 0.05 MPa) and UPy-Star (1.65 ± 0.11 MPa) films. In general, the UPy-Star poly(ethylene-co-propylene) exhibited improved

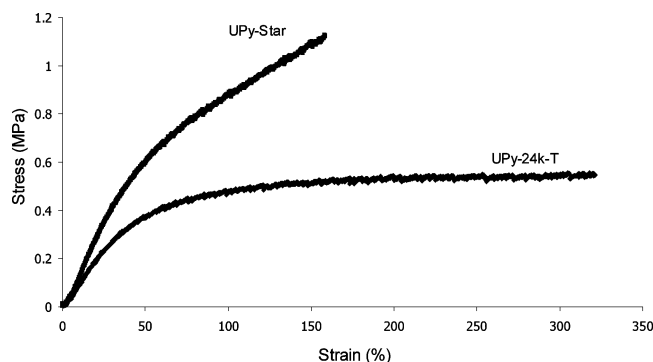


Figure 2. Stress–strain profiles for UPy-functionalized poly(ethylene-co-propylene)s, UPy-24K-T and UPy-star.

Table 4. Summary of Tensile Data for UPy-Functionalized Poly(ethylene-co-propylene)s, UPy-24K-T and UPy-Star

sample	modulus (MPa)	tensile strength at break (MPa)	% strain
UPy-24K-T	0.92 ± 0.05	0.56 ± 0.02	330 ± 59
UPy-Star	1.65 ± 0.11	1.06 ± 0.11	139 ± 37

tensile properties compared to the linear telechelic functionalized UPy-24K-T (Table 4).

Melt Rheological Characterization. Melt rheological characterization of well-defined nonfunctionalized and UPy-functionalized poly(ethylene-co-propylene)s and star-branched polymers revealed that high molecular weight star-branched architectures behaved very differently than lower molecular weight linear copolymers.

Viscosity vs temperature profiles for various UPy-modified poly(ethylene-co-propylene)s are shown in Figure 3. Monofunctional polymer (UPy-12K-mono) exhibited higher viscosity at low temperature and reached a consistent viscosity at ~ 80 °C. The telechelic functional polymers (UPy-12K-T and UPy-24K-T) exhibited higher viscosities than UPy-12K-mono and maintained significant viscosity at temperatures approaching 120 °C. The UPy-Star polymer, however, maintained significant viscosity to temperatures as high as 160 °C, which was attributed to more associations per star molecule (6 vs 2) and more thermal energy to disrupt the network-like structure.

Melt rheological data were compared for nonfunctionalized and UPy-functionalized linear and star polymers of precursor $M_n \sim 12\,000$ g/mol. While rheological data for the nonfunctionalized poly(ethylene-co-propylene)s obeyed time–temperature superposition (TTS) principles, it was observed that the loss modulus (G'') isotherms were not superimposable in the rubbery plateau region for the UPy-functionalized polymers. Thus, master curves were not constructed for UPy-functionalized polymers. TTS failure was attributed to the different temperature dependencies of the two mechanisms that governed the viscoelastic behavior of the polymer, i.e., the polymer relaxation and the hydrogen bond association/dissociation equilibrium. Other researchers have also observed similar TTS failure for G'' data that were obtained from melt rheological studies of multiple hydrogen bond containing polymers.^{75–77}

Figure 4 shows the dependence of dynamic storage moduli (G') on frequency at 50 °C for the nonfunctionalized and UPy-functionalized polymers. In the frequency range studied, both the nonfunctionalized linear and star-shaped poly(ethylene-co-propylene)s were in the terminal flow regime, where the star polymer exhibited a higher modulus compared to the linear counterpart consistent with a higher molecular weight for the star polymer. Significant differences were, however, observed between the nonfunctionalized and UPy-functionalized macro-

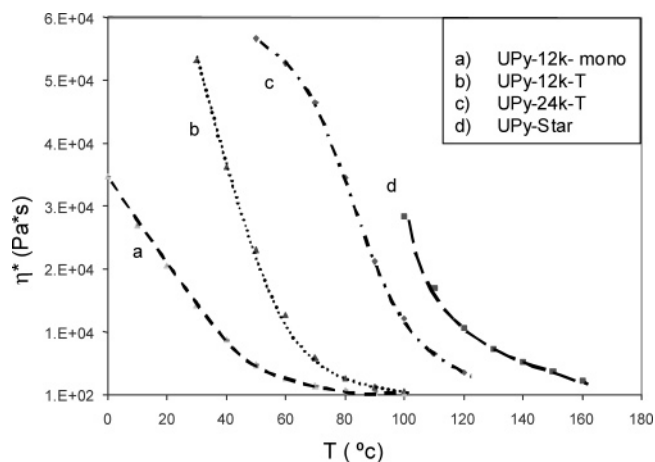


Figure 3. Dependence of complex viscosity on temperature for UPy-functionalized poly(ethylene-co-propylene)s of monofunctional (mono), telechelic (T), and star functionality: (a) UPy-12K-mono; (b) UPy-12K-T; (c) UPy-24K-T; (d) UPy-Star. Lines are drawn as a guide to the eye.

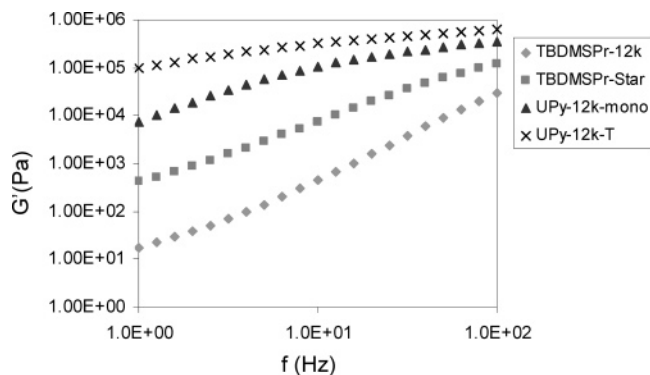


Figure 4. Dependence of storage moduli (G') on frequency at 50 °C for nonfunctionalized (TBDMSPr) and UPy-functionalized poly(ethylene-co-propylene)s of monofunctional (mono), telechelic (T) and star functionality: TBDMSPr-12K (diamonds); TBDMSPr-Star (squares); UPy-12K-mono (triangles); UPy-12K-T (crosses).

molecules. Both the UPy-functionalized polymers showed enhanced moduli with the presence of a rubbery plateau and transition to a terminal flow regime occurred at frequencies that were lower than those observed for the nonfunctionalized polymers. This indicated that the multiple hydrogen-bonding interactions in the case of UPy-functionalized polymers increased the apparent molecular weight and hindered chain reptation. UPy-12K-T exhibited a higher modulus and only a moderate transition to the terminal flow regime compared to UPy-12K-mono, which indicated the highest apparent molecular weight. It was previously proposed that telechelic functional polymers of this type exhibit end-to-end association in solution, with the resulting properties of a high-molecular-weight polymer, as shown in Figure 1b. It was postulated that the monofunctional UPy polymers formed aggregates in the melt, as shown in Figure 1a; however, larger scale aggregates were not formed due to only one functional end group. However, the presence of a terminal regime indicated that physical crosslinks were formed from reversible hydrogen-bonding interactions.⁷⁸

Figure 5 shows the dependence of complex viscosity (η^*) on frequency at 50 °C for the nonfunctionalized linear and star-shaped polymers as well as UPy-functionalized linear polymers. The nonfunctionalized polymers displayed typical Newtonian flow behavior characteristic of low-molecular-weight systems, which are below their entanglement molecular weight.⁷⁹ UPy-

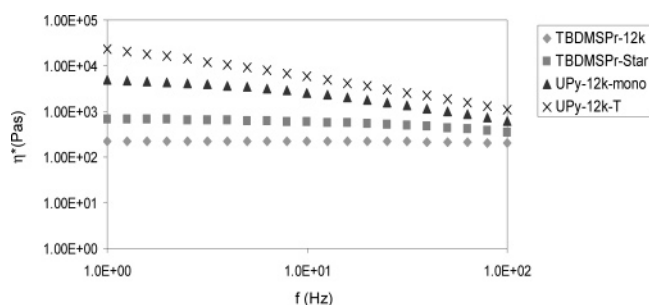


Figure 5. Dependence of complex viscosity on frequency at 50 °C for nonfunctionalized (TBDMSPr) and UPy-functionalized poly(ethylene-*co*-propylene)s of monofunctional (mono), telechelic (T), and star functionality: TBDMSPr-12K (diamonds); TBDMSPr-Star (squares); UPy-12K-mono (triangles); UPy-12K-T (crosses).

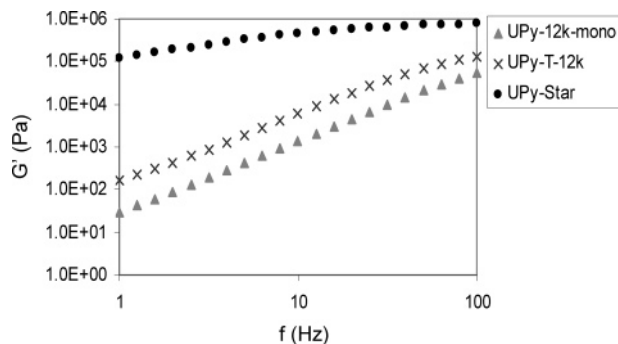


Figure 6. Dependence of storage moduli on frequency at 100 °C for UPy-functionalized poly(ethylene-*co*-propylene)s of monofunctional (mono), telechelic (T), and star functionality: UPy-12K-mono (triangles); UPy-12K-T (crosses); UPy-Star (circles).

functionalized polymers, however, showed a significant frequency dependence, which was attributed to strong multiple hydrogen-bonding interactions in the melt leading to a higher apparent molecular weight. The monofunctional polymer (UPy-12K-mono) exhibited shear thinning behavior while the telechelic polymer UPy-12K-T displayed non-Newtonian behavior in the frequency range studied. This observation suggested the formation of a highly entangled system. The presence of a Newtonian region in UPy-12K-mono and its absence in UPy-12K-T polymer indicated that fewer physical cross-links were present in the former, leading to a lower apparent molecular weight.

A common analysis temperature was not defined for the nonfunctionalized poly(ethylene-*co*-propylene)s and the UPy-Star polymer due to large differences in melt rheological behavior under these test conditions, and as a result, the nonfunctionalized linear and star-shaped poly(ethylene-*co*-propylene)s were not directly compared to the UPy-Star. Thus, the UPy-Star was only compared to both linear mono- and telechelic functional UPy polymers.

Figure 6 shows the dependence of storage moduli at 100 °C on frequency for a series of UPy-functionalized poly(ethylene-*co*-propylene)s. The linear samples UPy-12K-mono and UPy-12K-T were in the terminal flow regime. In contrast, UPy-Star exhibited an extended plateau regime and did not show significant transition to the terminal regime in the frequency range studied, which was attributed to physical cross-links as a result of multiple hydrogen-bonding interactions, as shown in Figure 1c.⁷⁶

Similarly, obvious differences were observed between the linear UPy-functionalized polymers and UPy-Star polymer in complex viscosity curves obtained at 100 °C (Figure 7). Both the mono- and telechelic UPy functional linear polymers showed

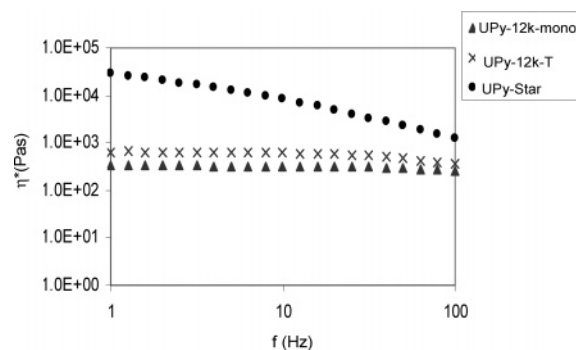


Figure 7. Dependence of complex viscosity on frequency at 100 °C for UPy-functionalized poly(ethylene-*co*-propylene)s of monofunctional (mono), telechelic (T) and star functionality: UPy-12K-mono (triangles); UPy-12K-T (crosses); UPy-Star (circles).

Newtonian behavior typical of low-molecular-weight polymers, while the UPy-Star sample exhibited shear thinning behavior. The presence of UPy functionality at each star terminus results in functionality greater than two and promotes long-range association through multiple hydrogen-bonding interactions.

Conclusions

The polymerization of isoprene was controlled using 3-(*tert*-butyldimethylsilyloxy)-1-propyllithium. Homopolymers with narrow molecular weight distributions were coupled efficiently with divinylbenzene to form star-shaped polymers. The polymers were subsequently hydrogenated and quantitatively deprotected to yield terminal hydroxyl functionality. The hydroxyl groups at the chain ends were functionalized via a two-step methodology to introduce UPy groups. Conversions, which ranged from 75 to 100%, were achieved for both linear and star-shaped poly(ethylene-*co*-propylene)s. DMA and DSC characterization revealed similar T_g 's for nonfunctionalized and UPy-functionalized polymers, and the values were in agreement with the expected value of -60 °C, for both linear and star-shaped polymers. In addition, UPy-Star exhibited an increased Young's modulus and decreased elongation at break compared to UPy-24K-T, which was consistent with a higher entanglement density for the star-shaped polymers.

In general, UPy-functionalized polymers exhibited significantly higher viscosities and extended plateau regime relative to nonfunctionalized analogues. This was attributed to the higher apparent molecular weight of the polymers with multiple hydrogen-bonding interactions, and telechelic functional polymers exhibited enhanced changes over monofunctional counterparts. UPy-Star polymer showed an extended rubbery plateau regime as well as an increase in the terminal relaxation time due to extensive association through multiple hydrogen-bonding interactions in comparison to linear UPy-functionalized counterparts. In addition, complex viscosity data further revealed the highly associated structure of the star-shaped UPy-functionalized polymer with non-Newtonian behavior in the low-frequency range.

Acknowledgment. This material is based upon work supported by the U.S. Army Research Laboratory and the U.S. Army Research Office under Contract/Grant DAAD19-02-1-0275 Macromolecular Architecture for Performance (MAP) MURI. The authors also thank FMC Corp. Lithium Division for donation of initiators.

Note Added after ASAP Publication. This article was published ASAP on March 30, 2006. The caption to Figure 5

has been modified. The correct version was posted on April 5, 2006.

References and Notes

- Long, V. C.; Berry, G. C.; Hobbs, L. M. *Polymer* **1964**, 5, 517.
- Burchard, W. *Adv. Polym. Sci.* **1999**, 143, 111.
- Mandelkern, L. *Crystallization of Polymers*; Cambridge University Press: New York, 2002; Vol. 1.
- Janzen, J.; Colby, R. H. *J. Mol. Struct.* **1999**, 485–485, 569.
- Hadjichristidis, N. *J. Polym. Sci., Part A: Polym. Chem.* **1999**, 37, 857.
- Tant, M. R.; Wilkes, G. L.; Storey, R. F.; Kennedy, J. P. *Polym. Bull. (Berlin)* **1985**, 13, 541.
- Wood-Adams, P. M.; Dealy, J. M.; deGroot, A. W.; Redwine, G. D. *Macromolecules* **2000**, 33, 7489.
- McKee, M. G.; Unal, S.; Wilkes, G. L.; Long, T. E. *Prog. Polym. Sci.* **2005**, 30, 507.
- Pakula, T.; Minkin, P.; Matyjaszewski, K. *ACS Symp. Ser.* **2003**, 854, 366.
- Hatada, K.; Kitayama, T.; Ute, K.; Nishiura, T. *J. Polym. Sci., Part A: Polym. Chem.* **2004**, 42, 416.
- Freire, J. J. *Adv. Polym. Sci.* **1999**, 143, 35.
- Hadjichristidis, N.; Fetters, L. J. *Macromolecules* **1980**, 13, 193.
- Bywater, S. *Adv. Polym. Sci.* **1979**, 30, 89.
- Tsoukatos, T.; Hadjichristidis, N. *J. Polym. Sci., Part A: Polym. Chem.* **2002**, 40, 2575.
- Quirk, R. P.; Yoo, T.; Lee, B. *J. Macromol. Sci., Pure Appl. Chem.* **1994**, 31, 911.
- Williamson, D. T.; Elman, J. F.; Madison, P. H.; Pasquale, A. J.; Long, T. E. *Macromolecules* **2001**, 34, 2108.
- Hirao, A.; Hayashi, M.; Tokuda, Y.; Haraguchi, N.; Higashihara, T.; Ryu, S. W. *Polym. J.* **2002**, 34, 633.
- Hadjichristidis, N.; Pitsikalis, M.; Pispas, S.; Iatrou, H. *Chem. Rev.* **2001**, 101, 3747.
- Meneghetti, S. P.; Lutz, P. J.; Rein, D. *Star-Shaped Polymers via Anionic Polymerization Methods*. In *Star and Hyperbranched Polymers*; Mishra, M.; Kobayashi, S., Eds.; Marcel Dekker: New York, 1999; p 27.
- Quirk, R. P.; Zhuo, Q.; Jang, S. H.; Lee, Y.; Lizarraga, G. *ACS Symp. Ser.* **1998**, 696, 2.
- Storey, R. F.; Shoemaker, K. A. *J. Polym. Sci., Part A: Polym. Chem.* **1999**, 37, 1629.
- Asthana, S.; Kennedy, J. P. *J. Polym. Sci., Part A: Polym. Chem.* **1999**, 37, 2235.
- Peetz, R. M.; Kennedy, J. P. *Macromol. Symp.* **2004**, 215, 191.
- Ingrisch, S.; Nuyken, O.; Mishra, M. K. *Plast. Eng.* **1999**, 53, 77.
- Charleux, B.; Faust, R. *Adv. Polym. Sci.* **1999**, 142, 1.
- Kennedy, J. P.; Jacob, S. *Acc. Chem. Res.* **1998**, 31, 835.
- Simms, J. A.; Spinelli, H. J. *Plast. Eng.* **1997**, 40, 379.
- Marsalko, T. J. *Macromol. Sci., Pure Appl. Chem.* **1997**, 34, 775.
- Pasquale, A. J.; Long, T. E. *J. Polym. Sci., Part A: Polym. Chem.* **2000**, 39, 216.
- Kamigaito, M.; Ando, T.; Sawamoto, M. *Chem. Rec.* **2004**, 4, 159.
- Hawker, C. J.; Bosman, A. W.; Harth, E. *Chem. Rev.* **2001**, 101, 3661.
- Sebenik, A. *Prog. Polym. Sci.* **1998**, 23, 875.
- Otsu, T.; Matsumoto, A. *Adv. Polym. Sci.* **1998**, 136, 75.
- Webster, O. W. *Makromol. Chem.* **1990**, 33, 133.
- Sivaram, S.; Lutz, P. J.; Mishra, M. K. *Plast. Eng.* **1999**, 53, 59.
- Jenkins, A. D. *Makromol. Chem., Macromol. Symp.* **1992**, 53, 267.
- Webster, O. W.; Sogah, D. Y. *Math. Phys. Sci.* **1987**, 215, 3.
- Quirk, R. P.; Jang, S. H.; Kim, J. *Rubber Rev., Rubber Chem. Technol.* **1996**, 69, 444.
- Hsieh, H. L.; Quirk, R. P. *Anionic Polymerization: Principles and Practical Applications*; Marcel Dekker: New York, 1996.
- Quirk, R. P.; Jang, S. H.; Yang, H.; Lee, Y. *Macromol. Symp.* **1998**, 132, 281.
- Quirk, R. P.; Jang, S. H.; Han, K.; Yang, H.; Rix, B.; Lee, Y. *Anionic Synthesis of Hydroxyl-Functionalized Polymers Using Protected, Functionalized Alkylolithium and Isoprenyllithium Initiators*. In *Functional Polymers*; 1998; Vol. 704, p 71.
- Quirk, R. P.; Mathers, R. T. *Polym. Bull. (Berlin)* **2001**, 45, 471.
- Switek, K. A.; Bates, F. S.; Hillmyer, M. A. *Macromolecules* **2004**, 37, 6355.
- Quirk, R. P.; Ma, J. J.; Lizarraga, G.; Ge, Q.; Hasegawa, H.; Kim, Y. J.; Jang, S. H.; Lee, Y. *Macromol. Symp.* **2000**, 161, 37.
- Hwang, J.; Foster, M. D.; Quirk, R. P. *Polymer* **2004**, 45, 873.
- Mizawa, T.; Takenaka, K.; Shiomi, T. *J. Polym. Sci., Part A: Polym. Chem.* **2000**, 38, 237.
- Tong, J.-D.; Zhou, C.; Ni, S.; Winnik, M. A. *Macromolecules* **2001**, 34, 696.
- Quirk, R. P.; You, F.; Wesdemiotis, C.; Arnould, M. A. *Macromolecules* **2004**, 37, 1234.
- Hedrick, J. L.; Trollsas, M.; Hawker, C. J.; Atthoff, B.; Claesson, H.; Heise, A.; Miller, R. D.; Mecerreyes, D.; Jerome, R.; Dubois, P. *Macromolecules* **1998**, 31, 8691.
- Cloutet, E.; Fillaut, J.-L.; Astruc, D.; Gnanou, Y. *Macromolecules* **1999**, 32, 1043.
- Coessens, V.; Pyun, J.; Miller, P. J.; Gaynor, S. G.; Matyjaszewski, K. *Macromol. Rapid Commun.* **2000**, 21, 103.
- Zhang, X.; Xia, J.; Matyjaszewski, K. *Macromolecules* **2000**, 33, 2340.
- Quirk, R. P. *Makromol. Chem., Macromol. Symp.* **1992**, 63, 259.
- Hayashi, M.; Kojima, K.; Hirao, A. *Macromolecules* **1999**, 32, 2425.
- Hirao, A.; Hayashi, M.; Haraguchi, N. *Macromol. Rapid Commun.* **2000**, 21, 1171.
- Hirao, A.; Hayashi, M.; Loykulant, S.; Sugiyama, K.; Ryu, S. W.; Haraguchi, N.; Matsuo, A.; Higashihara, T. *Prog. Polym. Sci.* **2005**, 30, 111.
- Bosman, A. W.; Vestberg, R.; Heumann, A.; Frechet, J. M. J.; Hawker, C. J. *J. Am. Chem. Soc.* **2003**, 125, 715.
- Ishizu, K.; Kitano, H.; Ono, T.; Uchida, S. *Polymer* **1999**, 40, 3229.
- Hadjichristidis, N.; Pispas, S.; Pitsikalis, M. *Prog. Polym. Sci.* **1999**, 24, 875.
- Pispas, S.; Floudas, G.; Hadjichristidis, N. *Macromolecules* **1999**, 32, 9074.
- Pispas, S.; Hadjichristidis, N. *Macromolecules* **2000**, 33, 6396.
- Pispas, S.; Hadjichristidis, N. *J. Polym. Sci., Part A: Polym. Chem.* **2000**, 38, 3791.
- Vlassopoulos, D.; Pitsikalis, M.; Hadjichristidis, N. *Macromolecules* **2000**, 33, 9740.
- Charalabidis, D.; Pitsikalis, M.; Hadjichristidis, N. *Macromol. Chem. Phys.* **2002**, 203, 2132.
- Sakellariou, G.; Pispas, S.; Hadjichristidis, N. *Macromol. Chem. Phys.* **2003**, 204, 146.
- Lange, R. F. M.; van Gurp, M.; Meijer, E. W. *J. Polym. Sci., Part A: Polym. Chem.* **1999**, 37, 3657.
- Yamauchi, K.; Lizotte, J. R.; Hercules, D. M.; Vergne, M. J.; Long, T. E. *J. Am. Chem. Soc.* **2002**, 124, 8599.
- Yamauchi, K.; Lizotte, J. R.; Long, T. E. *Macromolecules* **2002**, 35, 8745.
- Yamauchi, K.; Kanomata, A.; Inoue, T.; Long, T. E. *Macromolecules* **2004**, 37, 3519.
- Eckert, R. J. A. 4,156,673, 1979.
- Mays, J.; Hadjichristidis, N.; Fetters, L. J. *Macromolecules* **1984**, 17, 2723.
- Gotro, J. T.; Graessley, W. W. *Macromolecules* **1984**, 17, 2767.
- Brandrup, J.; Immergut, E. H.; Grulke, E. A. *Polymer Handbook*, 4th ed.; Wiley-Interscience: New York, 1999.
- Bikales, N. M. *Mechanical Properties of Polymers*; Wiley-Interscience: New York, 1971.
- Mueller, M.; Seidel, U.; Stadler, R. *Polymer* **1995**, 36, 3143.
- McKee, M. G.; Elkins, C. L.; Park, T.; Long, T. E. *Macromolecules* **2005**, 38, 6015.
- Fetters, L. J.; Graessley, W. W.; Hadjichristidis, N.; Kiss, A. D.; Pearson, D. S.; Younhouse, L. B. *Macromolecules* **1988**, 21, 1644.
- Hirschberg, J. H. K. K.; Beijer, F. H.; van Aert, H. A.; Magusin, P. C. M. M.; Sijbesma, R. P.; Meijer, E. W. *Macromolecules* **1999**, 32, 2696.
- Boils, D.; Perron, M.-E.; Monchamp, F.; Duval, H.; Maris, T.; Wuest, J. D. *Macromolecules* **2004**, 37, 7351.

MA052754+